



Connecting supernova remnants to their parent supernovae

S. Orlando¹, M. Miceli^{1,2}, F. Bocchino¹, and G. Peres^{1,2}

¹ Istituto Nazionale di Astrofisica – Osservatorio Astronomico di Palermo, Piazza del Parlamento 1, 90134 Palermo, Italy, e-mail: salvatore.orlando@inaf.it

² Dip. di Fisica e Chimica “Emilio Segrè”, Università di Palermo, Via Archirafi 36, 90123 Palermo, Italy

Received: 16 December 2021; Accepted: 31 May 2022

Abstract. This report summarizes the main results of a project funded under the agreement ASI-INAF n.2017-14-H.O. The aim has been to investigate fundamental problems concerning the physics of supernova remnants (SNRs), essential for a better understanding of: a) the dynamics of supernova (SN) engines, b) the latest stages of stellar evolution and c) the process of cosmic rays acceleration at shock fronts of SNRs. Our approach has been to develop detailed physical models describing the evolution from the SN to the SNR and to analyze high-energy observations of SNRs, using these models for an accurate interpretation of the data. Our studies have contributed to shed light on a number of long-standing issues in the field: how the final remnant morphology reflects the asymmetries developed in the immediate aftermath of the parent SN; how a highly inhomogeneous ambient environment affects the evolution and morphology of the remnants; how particles are heated and accelerated by the shocks in SNRs.

Key words. magnetohydrodynamics – instabilities – shock waves – ISM: supernova remnants – X-rays: ISM – cosmic rays

1. Introduction

Supernova remnants (SNRs), the outcome of supernova (SN) explosions, are extended sources with complex morphologies and non-uniform distributions of ejecta. Such properties reflect asymmetries developed soon after the parent SN explosion and the effects of interaction of the SN blast wave with the inhomogeneous circumstellar medium (CSM). Thus, investigating the link between SNRs and their parent SNe may help: 1) to trace back the characteristics of the asymmetries occurred during the SN, providing a physical insight into

the processes governing the SN engines; 2) to probe the structure of the CSM surrounding the SN, thereby mapping the mass loss history of the progenitor stars in the final stages of their evolution. In the last years, our group has started a program aimed at bridging the gap between SNe and SNRs and based on the comparison of 3D magnetohydrodynamic (MHD) simulations with multi-wavelength observations. First pioneering studies have demonstrated that our approach can be very effective in gaining a deep physical insight of the phenomena occurred soon after the SN (Orlando et al. 2015, 2016).

In the framework of a project funded under the agreement ASI-INAF n.2017-14-H.O, we extended our previous studies by coupling 3D SNR models with 3D core-collapse SN models that include the most important ingredients to describe the complex phases in the SN evolution and the subsequent expansion of the blast wave through the inhomogeneous and magnetized CSM. We performed 3D MHD simulations that describe the complete evolution from the core-collapse to the full-fledged SNRs of specific objects and we analyzed X-ray observations of SNRs, using the models for the interpretation of the data, when possible. Here, we summarize some of the main results achieved.

2. Three-dimensional MHD modeling

2.1. Effects of SN anisotropies

We performed an extensive campaign of 3D MHD simulations which describe the evolution of a core-collapse SN from its explosion to the expansion of its remnant for 5000 yr (Tutone et al. 2020). The aim has been to investigate how post-explosion ejecta anisotropies influence the structure and chemical properties of the remnant at later times. We found that large-scale anisotropies developed soon after the core-collapse can strongly modify the chemical stratification in the ejecta, leading to spatial inversion of ejecta layers (for instance, leading to Fe/Si-rich ejecta outside the O shell) or the formation of Fe/Si-rich jet-like features that may protrude the remnant outline. All these features are revealed in some SNRs, so that they can be signatures of post-explosion anisotropies. We suggest that the comparison between models and observations can help to probe the early phases of SN explosions.

We also performed 3D MHD simulations to study two popular young SNRs: SN 1987A and Cassiopeia A (Cas A). For the first SNR, the aim has been to link the dynamical and radiative properties of the remnant to the geometrical and physical characteristics of the parent SN and to the nature of its progenitor star. We performed 3D simulations of an aspherical SN, initialized from pre-SN stellar models available in the literature and includ-

ing all physical processes necessary to describe the evolution of the blast wave from the core-collapse to the breakout of the shock wave at the stellar surface (Ono et al. 2020). The output of these simulations has been used as initial condition for the structure and chemical composition of ejecta in 3D MHD simulations which describe the subsequent interaction of the remnant with the highly inhomogeneous CSM around SN 1987A (Orlando et al. 2020). The comparison of model results with multi-wavelength observations revealed that: 1) the high mixing of ejecta detected in observations of SN 1987A require a highly asymmetric SN explosion; 2) the observed distribution of ejecta and the dynamical and radiative properties of the SNR suggest that the progenitor star was a blue supergiant generated by the merging of two massive stars.

As for Cas A, the aim has been to investigate if and how the remnant still keeps memory of the asymmetries that developed stochastically during the first second of the SN explosion after core bounce. To this end, 3D MHD simulations of the SNR were coupled to a 3D hydrodynamic model of a neutrino-driven SN explosion (Wongwathanarat et al. 2017). The SN-SNR simulations include all physical processes relevant to describe the complexities in the SN evolution and the subsequent interaction of the stellar debris with the wind of the progenitor star (Orlando et al. 2021b). Large-scale asymmetries originate from the earliest phases of the explosion due to hydrodynamic instabilities in the neutrino-heating layer (convective overturn and the standing accretion shock instability; SASI). We demonstrated that the interaction of these asymmetries with the reverse shock produces, at the age of ≈ 350 yr, a remnant morphology and distribution of ejecta which are remarkably similar to those observed in Cas A (see Fig. 1; Orlando et al. 2021b): a pattern of ring- and crown-like structures of shocked ejecta, the spatial inversion of the ejecta layers with Si-rich ejecta physically interior to Fe-rich ejecta, the voids and cavities in the innermost unshocked ejecta, the asymmetric distributions of ^{44}Ti and ^{56}Fe .

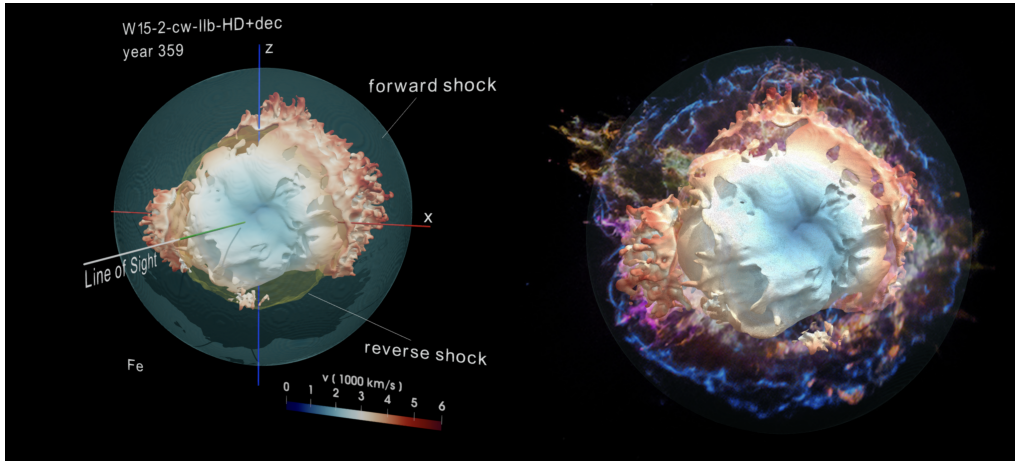


Fig. 1. Distribution of iron in the remnant of a neutrino-driven SN explosion derived from the model W15-2-cw-IIb-HD+dec (Orlando et al. 2021b). Left panel: The colored isosurface marks the distribution of iron after 359 years of evolution (nearly the age of the SNR Cas A). The opaque irregular isosurface corresponds to a value of Fe density which is at 5% of the peak density; the colors give the radial ejecta velocity in units of 1000 km s^{-1} on the isosurface (the color coding is defined at the bottom of the panel). The semi-transparent quasi-spherical surfaces indicate the forward (green) and reverse (yellow) shocks. The Earth vantage point lies on the negative y -axis. Right panel: comparison between the modeled distribution of Fe-rich ejecta (represented as in the left panel) with observations of Cas A; the transparent image passing through the center of the remnant is a composite showing optical (Hubble) and X-ray (Chandra) actual observations of the remnant. Interactive 3D graphics of this model are available at the links <https://skfb.ly/6TKRK> and <https://skfb.ly/o8r7V>.

2.2. Effects of an inhomogeneous CSM

The simulations performed for SN 1987A allowed us also to investigate the effects of a highly inhomogeneous CSM onto the morphology of the remnant (Orlando et al. 2020). The comparison of model results with observations enabled us to reconstruct the geometry and density distribution of the material in the CSM around SN 1987A, providing constraints on the mass loss history of the progenitor system (see Fig. 2).

Other 3D hydrodynamic simulations have investigated the origin of the complex morphology and X-ray emission observed in the SNR IC 443 (Ustamujic et al. 2021). The aim has been to explore the effects of the inhomogeneous ambient medium in shaping the observed structure of IC 443 and to derive the main parameters characterizing the remnant. We performed 3D hydrodynamic simulations which described the interaction of

the SNR with the inhomogeneous environment, parameterized in agreement with the results of the multi-wavelength data analysis (see Sect. 3.2). The exploration of the parameter space has shown that (see Fig. 3): 1) the complex centrally-peaked X-ray morphology of IC 443 can be naturally explained by the interaction of the remnant with the cloudy environment in which the remnant expands; 2) the origin of the explosion coincides with the position where the pulsar wind nebula (PWN) CXOU J061705.3+222127 was at the time of the explosion (see also Sect. 3.2); 3) the mass of the ejecta is $\approx 7 M_{\odot}$, the energy of the explosion is $\approx 10^{51}$ erg and the age of the remnant is ≈ 8000 yr.

2.3. Particle acceleration and non-thermal emission

Our simulations were also used to investigate the signatures of cosmic rays acceleration and

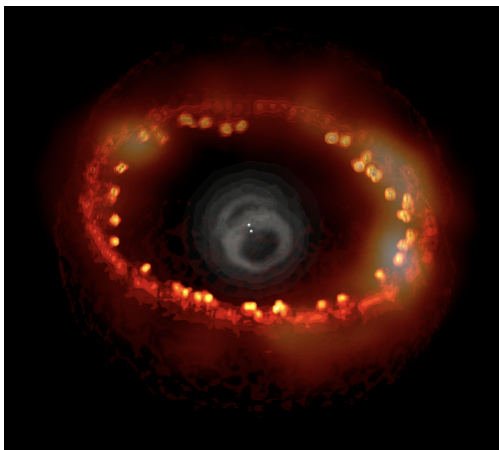


Fig. 2. X-ray emission expected for SN 1987A 30 years after the SN event as synthesized from the model B18.3 presented in Orlando et al. (2020). The X-ray emission is produced during the interaction of the blast wave from SN 1987A and the inhomogeneous CSM characterized by a dense ring of material. During the interaction, the gas is heated up to temperatures of millions degrees and emits X-rays. In dark-red the less intense X-ray emitting regions, in yellow the most intense. The yellow blobs are due to shocked clumps of the ring around the SN that formed well before the SN explosion due to the winds of the progenitor star. The semitransparent panel superimposed to the model shows the actual Chandra observation of SN 1987A; 3D spatial distribution of the absorbing cold ejecta (white structure in the center of the remnant) reconstructed from the model is also shown. The center of the explosion and the position of the pulsar as predicted by the model are indicated by the 2 dots close to the center (see also Greco et al. 2021). An interactive 3D graphics of this model is available at the link <https://skfb.ly/6YNNE>.

to put constraints on the acceleration mechanism of high energy particles (Orlando et al. 2021a). In particular, we investigated the process of particle acceleration during the transition from the phase of SN to that of SNR, considering again the case of SN 1987A. We studied the evolution of this object from the immediate aftermath of the core-collapse of the progenitor star to the subsequent interaction of its remnant with the nebula, synthesizing its thermal X-ray emission and non-thermal

radio emission (Orlando et al. 2019a). From the comparison of model results with observations, we found that: 1) the radio emission originates mostly from the forward shock traveling through the H II region; 2) the non-thermal radio flux from the reverse shock is heavily suppressed; 3) synchrotron self-absorption and free-free absorption have negligible effects on the emission during the interaction with the nebula. We concluded that the emission from the reverse shock at radio frequencies might be limited by highly magnetized ejecta.

3. Analysis of X-ray observations

3.1. Collisionless shock heating of heavy ions

Among other things, the 3D MHD simulations presented in Sect. 2 were used to interpret X-ray observations of SNRs and to extract information on the physical processes governing the evolution and structure of these extended objects. More specifically, we analyzed spectra collected with the Chandra X-ray telescope (Miceli et al. 2019) through 3D simulations, describing the evolution of SN 1987A from the SN explosion to the interaction of the blast wave with the inhomogeneous CSM (Orlando et al. 2015, 2019a). The aim has been to investigate the physics of collisionless shocks, namely shocks with a thickness of their jump much shorter than the collisional mean free path. An important property of these shocks is that electrons, protons and ions are expected to be heated at different temperatures when they cross the shock front. The actual dependence of the post-shock temperature on the particle mass is, however, still widely debated.

The case of SN 1987A is particularly interesting to investigate the issue of particle heating because the remnant is very young (about 30 years old), the shock is relatively fast and interacts with a high density nebula in the CSM (leading to a bright emission from the post-shock plasma). We developed a novel approach for the data analysis which is based on the close comparison between the multi-epoch, high-resolution X-ray spectra collected with Chandra with the 3D simulations describ-

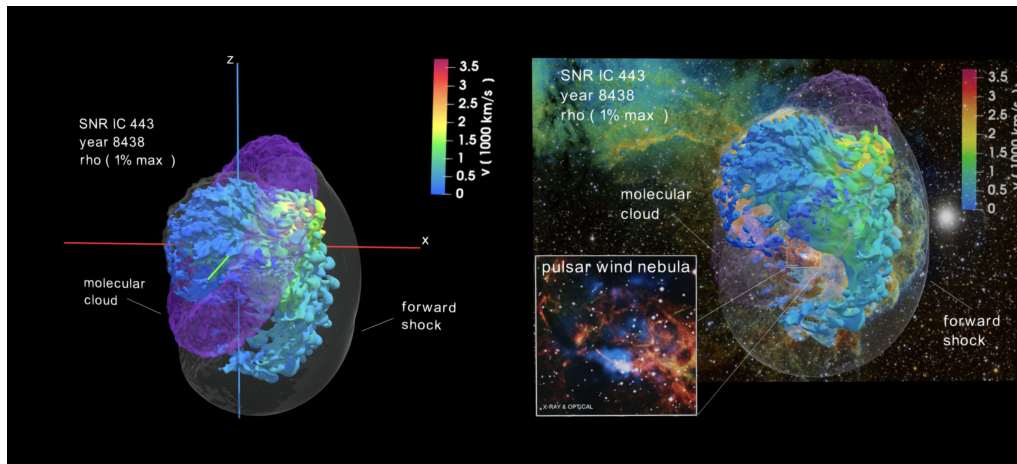


Fig. 3. Distribution of stellar debris (ejecta) in the SNR IC 443 as derived from HD simulations (Ustamujic et al. 2021). Left panel: the colored isosurface shows the distribution of the ejecta approximately 8400 years after the SN explosion. This isosurface corresponds to a density value which is at 1% of the peak density; the colors give the radial velocity in units of 1000 km s^{-1} on the isosurface. The outer semi-transparent surface marks the position of the forward shock; the toroidal semi-transparent structure in purple represents a molecular cloud of the interstellar medium with which the blast wave of the remnant interacts. The line of sight lies in the negative y -axis. Right panel: comparison of the modeled SNR (represented as in the left panel) with observations. The transparent image passing through the center of the remnant is a wide field optical observation of the remnant (Bob Franke; Focal Pointe Observatory). The inset box shows a composite optical (red, yellow; DSS, SARA) and X-ray (blue; D. Swartz NASA/CXC/MSFC) observation of the PWN CXOU J061705.3+222127. Interactive 3D graphics of this model are available at the links <https://skfb.ly/6W9oM> and <https://skfb.ly/6X6BV>.

ing SN 1987A. The synthesis of X-ray spectra from the models self-consistently accounts for the broadening of spectral lines of many ions together. Thanks to our approach, we were able to disentangle the Doppler broadening of the emission lines due to plasma velocity along the line of sight from the thermal broadening of the same lines. From the latter, we were able to measure the post-shock temperature of protons and ions of a selected sample of emission lines from different ion species. We found that the ratio of ion temperature to proton temperature is always significantly higher than one and increases linearly with the ion mass for a wide range of masses and shock parameters. Our findings were recently confirmed from the analysis of new Chandra observations of SN 1987A (Ravi et al. 2021).

3.2. Origin of recombining plasma

In the framework of the project, we also investigated the origin of overionized recombining plasmas in mixed-morphology (MM) SNRs. We analyzed X-ray observations of two remnants belonging to this class: IC 443 and W44. In both cases, we analyzed their XMM-Newton observations and performed a spatially resolved spectral analysis of their X-ray emission. In the case of IC 443, we identified a jet-like Mg-rich structure of recombining plasma, possibly resulting from the adiabatic expansion of the ejecta (Greco et al. 2018). We found that the jet is aligned with the position, at the time of SN explosion, of a PWN apparently within the remnant. In the light of the match between the jet's direction and the position of the PWN, we suggested that the PWN might be the relic of the IC 443 progenitor star.

In the case of W44, we found a clear anticorrelation between the electron temper-

ature and the recombination timescale in regions interacting with dense molecular clouds (Okon et al. 2020). We interpreted the result as evidence of recombining plasma resulting from the rapid cooling through thermal conduction with the dense and cold clouds interacting with the remnant. Thus, we suggested that the plasma cooling by thermal conduction can contribute to the production of overionization in SNRs in addition to the adiabatic expansion.

4. Conclusions

Our studies have demonstrated that accurate modeling of SNRs can be very effective in disentangling the effects from initial interior inhomogeneities (from the SN explosion) and asymmetries from CSM effects and can provide clues on the nature of the progenitor systems. The comparison of model results with observations of SNRs, therefore, can be a valuable tool to probe: 1) the physics of SN engines; 2) the structure and geometry of the CSM, providing hints on the latest phases of evolution of the progenitor systems; 3) the role played by SNRs in the heating and acceleration of particles crossing the shocks.

Acknowledgements. We acknowledge partial financial contribution from the agreement ASI-INAF n.2017-14-H.O. We are grateful to E. Greco, H.-T. Janka, S. Nagasaki, M. Ono, A. Tutone, S. Ustamujic, A. Wongwathanarat for their fundamental contribution to the success of the project. The navigable 3D graphics have been developed in the framework of the project 3DMAP-VR (3-Dimensional Modeling of Astrophysical Phenomena in Virtual Reality; Orlando et al. 2019b) at INAF-Osservatorio Astronomico di Palermo.

References

- Greco, E., Miceli, M., Orlando, S., et al. 2021, *ApJ*, 908, L45
- Greco, E., Miceli, M., Orlando, S., et al. 2018, *A&A*, 615, A157
- Miceli, M., Orlando, S., Burrows, D. N., et al. 2019, *Nature Astronomy*, 3, 236
- Okon, H., Tanaka, T., Uchida, H., et al. 2020, *ApJ*, 890, 62
- Ono, M., Nagasaki, S., Ferrand, G., et al. 2020, *ApJ*, 888, 111
- Orlando, S., Miceli, M., Petruk, O., et al. 2019a, *A&A*, 622, A73
- Orlando, S., Miceli, M., Pumo, M. L., & Bocchino, F. 2015, *ApJ*, 810, 168
- Orlando, S., Miceli, M., Pumo, M. L., & Bocchino, F. 2016, *ApJ*, 822, 22
- Orlando, S., Miceli, M., Ustamujic, S., et al. 2021a, *New Astronomy*, 86, 101566
- Orlando, S., Ono, M., Nagasaki, S., et al. 2020, *A&A*, 636, A22
- Orlando, S., Pillitteri, I., Bocchino, F., Daricello, L., & Leonardi, L. 2019b, *Research Notes of the American Astronomical Society*, 3, 176
- Orlando, S., Wongwathanarat, A., Janka, H. T., et al. 2021b, *A&A*, 645, A66
- Ravi, A. P., Park, S., Zhekov, S. A., et al. 2021, *ApJ*, 922, 140
- Tutone, A., Orlando, S., Miceli, M., et al. 2020, *A&A*, 642, A67
- Ustamujic, S., Orlando, S., Greco, E., et al. 2021, *A&A*, 649, A14
- Wongwathanarat, A., Janka, H.-T., Müller, E., Pllumbi, E., & Wanajo, S. 2017, *ApJ*, 842, 13